Self-accommodating honeycomb networks from supramolecular selfassembly of s-indacene-tetrone on silver surfaces

Nataliya Kalashnyk, Sylvain Clair

▶ **To cite this version:**

Nataliya Kalashnyk, Sylvain Clair. Self-accommodating honeycomb networks from supramolecular selfassembly of s-indacene-tetrone on silver surfaces. Langmuir, 2022, 38 (3), pp.1067-1071. 10.1021/acs.langmuir.1c02640 . hal-03585485

HAL Id: hal-03585485
https://hal.science/hal-03585485v1

Submitted on 23 Feb 2022

HAL is a multi-disciplinary open access archive for the deposit and dissemination of scientific research documents, whether they are published or not. The documents may come from teaching and research institutions in France or abroad, or from public or private research centers.

L'archive ouverte pluridisciplinaire **HAL**, est destinée au dépôt et à la diffusion de documents scientifiques de niveau recherche, publiés ou non, émanant des établissements d'enseignement et de recherche français ou étrangers, des laboratoires publics ou privés.

Self-accommodating honeycomb networks from supramolecular self-assembly of *s*-indacene-tetrone on silver surfaces

Nataliya Kalashnyk, Sylvain Clair*

Aix Marseille Univ, CNRS, IM2NP, Marseille, France

* Corresponding author: S. Clair, sylvain.clair@cnrs.fr

Abstract:

We describe the self-assembly of *s*-indacene-tetrone on the Ag(111), Ag(100) and Ag(110) surfaces and the formation of three hydrogen-bonded supramolecular phases representing complex self-accommodating honeycomb network. The differences in terms of relative host-guest stability and molecular density are analyzed and discussed. Different epitaxial behaviors of the 2D self-assembly are found as a response to the variations in the crystallographic orientation of the surface.

INTRODUCTION

Supramolecular self-assembly of small planar aromatic molecules at surfaces can provide a tremendous variety of nanostructures by taking advantage of weak and reversible intermolecular interactions, as revealed at the single molecule level by scanning probe microscopy.[1-5] Among the various tessellation patterns that can be created, the honeycomb network is particularly attractive due to its nanoporosity[2,6,7] leading to confinement effects[8] or potentially representing a prototypical system of host-guest molecular complexes.[9-11] In some cases, the system can be self-accommodating, i.e. incorporate some of the frame molecules (host) as guest,[12-14] as it is the case occasionally for example with the various porous networks formed by trimesic acid.[15-17] In this work we were interested in a particular type of self-accommodating honeycomb network, for which the nanopores are systematically filled in a periodic fashion. In the resulting complex hierarchical patterning, the guest molecules are getting entirely involved in the self-assembly of the honeycomb framework and contribute to the stability of the whole pattern. This model system could be modulated by changing the crystallographic orientation of the supporting surface. We show that a different behavior can be observed in terms of the relative stability of the host and the guest systems. In particular, a molecular switch was created.

The molecule of choice is *s*-indacene-1,3,5,7(2*H*,6*H*)-tetrone ($INDO_4$, see inset in Fig. 1)[18,19] and is constituted of a small indacene backbone surrounded by four oxygen atoms with D2h symmetry, thus presenting a highly favourable configuration to establish various intermolecular in-plane hydrogen bonds.[20] A variety of different ordered phases can be obtained upon room-temperature deposition of $INDO_4$ on silver surfaces, eventually upon mild annealing, as reported previously. [21,22] Covalent coupling involving complex and diverse reaction pathways has been also demonstrated with this molecule upon high temperature annealing.[21,23]

Room-temperature scanning tunneling microscopy (STM) investigations in ultrahigh vacuum (UHV) were conducted on the $INDO_4$ precursor adsorbed on silver surfaces. We show that this molecule self-assembles into three different self-accommodating honeycomb structures on the Ag(111), Ag(100) and Ag(110) surfaces. The formation of these supramolecular networks is driven by a balance between molecule-substrate and intermolecular hydrogen-bonds originating from the presence of several O and H peripheral atoms in the precursor. All three periodic structures found at sub-monolayer coverage can be described by large unit cells containing six indacenes. The discrimination between the honeycomb host molecules and the guests is revealed by the two different contrasts appearing in the STM images. Contrary to other host-guest systems,[9-13,15-17] the corresponding empty honeycomb frameworks were never observed, which indicates a probable important interdependence between both molecular types.

RESULTS AND DISCUSSION

HC1 on Ag(100):

A variety of different structures can be formed upon deposition of $INDO_4$ on Ag(100) depending on the annealing temperature, as reported previously.[21,22] The extended ordered phase HC1 is obtained by gentle annealing to a temperature of 80 °C (Fig. 1). STM images show a complex pattern of bright elongated features corresponding to the dimension of the $INDO_4$ molecule. The unit cell (**a**,**b**) is quasi-rectangular and includes 6 molecules. This phase can be regarded as a filled honeycomb network where individual molecules (type A) are enclosed in a honeycomb framework cavity formed by 6 molecules (type B). This description is inspired by the different contrast between A and B molecules occasionally observed depending on the tip conditions (ESI Fig. S1). The type B1 and B2 molecules have their long axis coinciding respectively with the $[011]$ and $[0\bar{1}1]$ close-packed directions of the underlying surface, while the type A1 and A2 molecules form an angle of ±25° with these directions. As a result, the unit cell includes two distinct honeycomb cavities, with distinct chirality so that both honeycomb motifs within a unit cell are mirror symmetric.

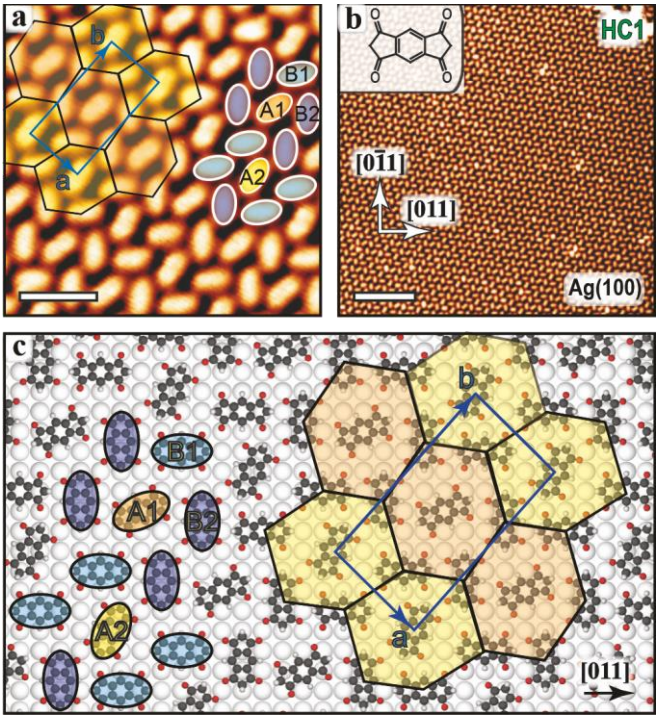

Figure 1: *(a,b) STM images of the self-accommodating honeycomb supramolecular phase HC1 formed by INDO$_4$ on Ag(100). (c) Corresponding adsorption model. Ag surface atoms are represented as light grey spheres. Scale bars: (a) 2 nm, (b) 8 nm. The molecular structure of INDO$_4$ is sketched in inset in (b).*

Point defect inside the domains are rare and limited to individual molecule with different contrast (Fig. 2a). The island perimeters are terminated non-specifically by types A and B molecules (see Fig. 2d). This observation suggests that the adsorption of both type A and B configurations might be energetically equivalent in this tiling pattern.

Anticipated adsorption sites and intermolecular interactions can be estimated by carefully overlapping scaled ball-and-stick models of INDO$_4$ with the experimental STM images. The final molecular assembly is afterwards placed above the atomic model of the silver surface in such a way that all O atoms of the molecules in the network would be located as close as possible to on-top sites of the Ag substrate, by analogy with the configuration that was observed for other similar molecules.[24,25] A tentative model of the self-assembly is shown in Fig. 1c. The different adsorption configurations of type A and B molecules are in agreement with the specific STM contrast occasionally observed (see ESI Fig. S1b). More specifically, the frame molecules (B1 and B2) can also exhibit two levels of brightness depending on their orientation along $[0\bar{1}1]$ or $[011]$ direction (ESI Fig. S1c), in agreement with the different adsorption sites for B1 and B2 in the model. A (4 -4; 7 8) superlattice can be derived for this molecular assembly including 2 filled honeycomb cavities and 6 molecules per unit cell (lattice vectors $|\mathbf{a}|$ = 5.7 Å, $|\mathbf{b}|$ = 10.6 Å, $\angle\mathbf{a},\mathbf{b}$ = 86°). The density of this phase is thus 1.20 molecule.nm^{-2}. Note that, due to the symmetry mismatch with the square Ag(100) surface, the filled honeycomb has a slightly distorted geometry because a perfect honeycomb network would deliver $\angle\mathbf{a},\mathbf{b}$ = 90° and $|\mathbf{b}|/|\mathbf{a}| = \sqrt{3} \approx 1.73$ while we have here $\angle\mathbf{a},\mathbf{b}$ = 86° and $|\mathbf{b}|/|\mathbf{a}|$ = 1.86.

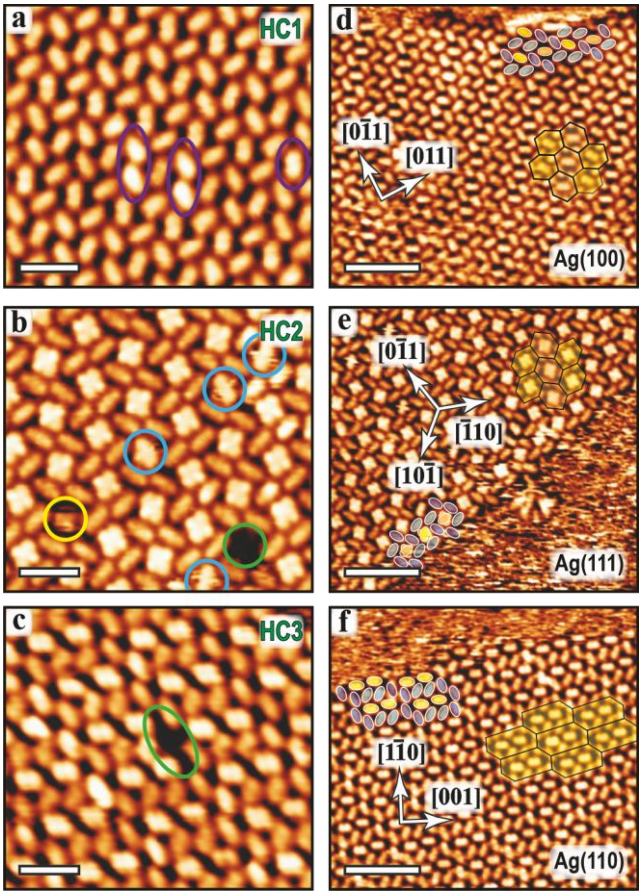

Figure 2: *STM images of the point and vacancy defects (a-c) and of the island perimeters (d-f) of the (a,d) HC1, (b,e) HC2 and (c,f) HC3 phases formed on Ag(100), Ag(111) and Ag(110), respectively. Scale bars: (a-c) 2 nm, (d-f) 5 nm.*

HC2 on Ag(111):

We could similarly observe two other types of filled honeycomb networks on other silver surfaces exhibiting different crystallographic structures. On Ag(111) a variety of different structures can be formed depending on the annealing temperature, as reported previously.[21,22] Annealing to a temperature of 200°C, close to the reaction temperature, leads to the formation of the extended ordered phase HC2 (Fig. 3a). This close-packed structure is composed of two distinct characteristic contrasts. Bright square features (type A) are enclosed in a honeycomb framework cavity formed by six dimmer elongated features (type B). The latter are similar to those observed in HC1 and correspond to the dimension of an individual $INDO_4$ molecule. A close-up image in Fig. 3b reveals that the long axis of the type B molecules makes an angle of ±40° with respect to the close packed [$\bar{1}$10] direction. The square type A features present two distinct orientations A1 and A2 alternating within neighboring honeycomb framework cavities. As a result, the unit cell of this structure includes two equivalent honeycomb cavities with distinct chirality. The unit cell is rectangular and includes 4 framework molecules B and 2 type A features. The close-up image in Fig. 3b reveals that the latter display a cross-like contrast which diagonal length is matching well the dimension of an $INDO_4$ molecule. Based on these observations, and by analogy with the HC1 network on Ag(100) described above we can postulate that the type A correspond to single molecules that are trapped within the honeycomb framework cavities and that can freely rotate between two metastable positions that are 90° rotated

with respect to each other. As a result, the apparent square-shaped STM contrast corresponds to the average occupation position, similar to other studies displaying dynamical systems.[13,26,27]

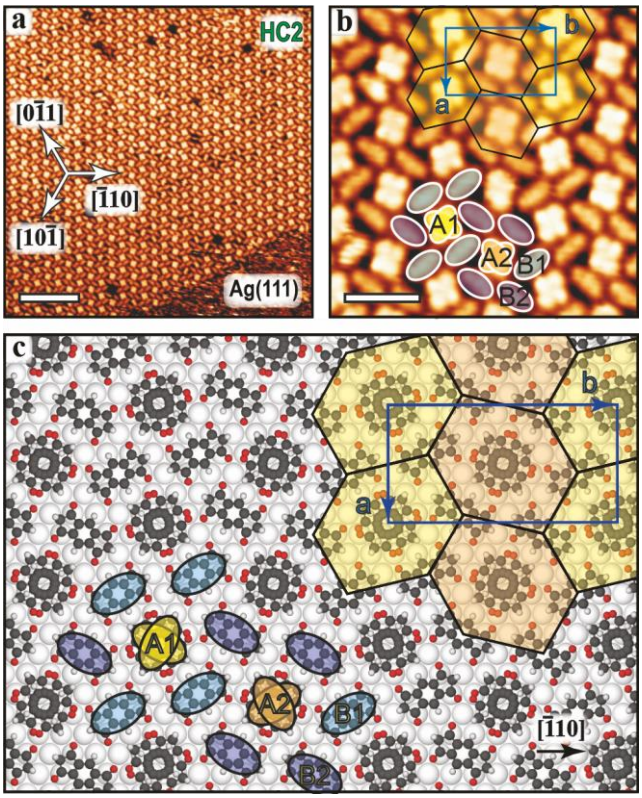

Figure 3: *(a,b) STM images of the self-accommodating honeycomb supramolecular phase HC2 formed by $INDO_4$ on Ag(111). (c) Corresponding adsorption model. Ag surface atoms are represented as light grey spheres. Scale bars: (a) 8 nm, (b) 2 nm.*

Careful inspection of the vacancy defects within this structure allowed confirming the presence of only one molecule per cavity. As highlighted by the colored circles in Fig. 2b, defects are preferentially found inside the cavities and appear as empty (green) or fuzzy pores (yellow), as well as single elongated bright STM feature of the same shape and dimension as type B ones, but still with different molecular contrast (blue circles). Indeed, these vacancy defects are not static and dynamic processes occur between them (ESI Fig. S2).[28] Moreover the defective type A visualized as a single elongated bright protrusion keeps the orientation corresponding to one of the diagonals of the initial bright cross-feature, distinct from the orientation of type B molecules (see ESI Fig. S2a). This supports the evidence that the cross-like STM features are single molecules rotating between two perpendicular metastable orientations. Furthermore, it gives a hint on the higher stability of type B molecules forming the honeycomb framework as compared to type A molecules accommodated inside the cavities. This assumption is also supported by the observation of the perimeter region of the domains. As shown in Fig. 2e, the edges of the molecular islands are preferentially terminated by the more stable type B molecules.

Here again we can propose a tentative model of the self-assembled pattern in Fig. 3c. The rectangular unit cell of this molecular assembly includes 6 molecules forming a (3 -6; 10 0) superlattice unit cell (lattice vectors vectors $|\mathbf{a}|$ = 5.2 Å, $|\mathbf{b}|$ = 10.0 Å, $\angle\mathbf{a},\mathbf{b}$ = 90°). The different adsorption configurations of type A and B molecules are in agreement with the different STM contrast. The density is estimated to 1.38 molecule.nm^{-2}. The higher density of this phase as compared to that of HC1 (1.20 molecule.nm^{-2}) could be responsible for the creation of some compressive strain within the honeycomb cavities

inducing the metastable configuration of the type A molecules. Despite the threefold symmetry of the surface, a fourfold symmetry of the rotating molecules is observed. This suggests that mainly intermolecular interactions are responsible for the dynamic behavior. In fact a repulsive component between the oxygen atoms of neighboring molecules is expected because it appears that the inside of the honeycomb pores is predominantly surrounded by oxygen atoms, see model Fig. 3c. The low stability of the rotating molecules is further evidenced by the island terminations of preferential type B framework molecules.

HC3 on Ag(110):

With regard to the two phases presented above, the case of another HC3 phase on Ag(110) can be comparatively discussed. This phase has been previously described[23] and is obtained in extended fashion by moderate annealing (50 °C), see Fig. 4a. Two distinct bright (type A) and dim (type B) features are observed, the size of which corresponds to the dimension of individual $INDO_4$ molecules. An inverted contrast is occasionally observed depending on the tip conditions (see ESI Fig. S3). The long axis of type B molecules is rotated by an angle of ±25 ° with respect to the close-packed $[1\bar{1}0]$ direction, while that of the type A molecules coincides with the [001] surface direction. The motif formed by the arrangement of the type B molecules can be regarded as a distorted honeycomb framework, i.e. elongated in one direction. The cavities formed by 10 type B molecules are accommodating 2 type A molecules. As compared with the other HC1 and HC2 honeycomb frameworks, all cavities are identical but twice larger, thus the unit cell is composed similarly of 6 molecules.

The island edges and the presence of vacancy defects in HC3 on Ag(110) were examined to define which of the A or B molecule type is more stable. Surprisingly, a completely reverse situation is found here. As illustrated in Figs. 2c and 2f, the type A [001]-oriented molecules are mainly decorating the island edges while in island interior the occasional absence of type B molecules in the honeycomb framework constitutes the main vacancy defect type. Thus, type A molecules appear to be more stable with possibly stronger surface interaction.

The tentative model of the HC3 pattern is shown in Fig. 4c. The different adsorption configurations of type A and B molecules are in agreement with the different STM contrast. In this model, the four O atoms of type A molecules are lying favorably close to on-top sites of Ag substrate providing a possible explanation for their higher stability over the type B indacenes. The molecular network can be described by a (5 -2; 5 6) superlattice comprising 6 molecules per unit cell (lattice vectors $|\mathbf{a}|$ = 5.74 Å, $|\mathbf{b}|$ = 9.85 Å, $\angle\mathbf{a},\mathbf{b}$ = 89°). The density of HC3 is thus 1.27 molecule.nm^{-2}, of intermediate level between HC1 and HC2.

The distorted doubly-filled framework of HC3 can actually be regarded as the lateral fusion of neighboring pores of a singly-filled regular honeycomb framework, as shown in Fig. 4d. It is in principle possible to make a (virtual) transformation from a regular honeycomb framework to the HC3 structure by performing limited displacement of the framework positions. As compared to HC1, such transformation can slightly increase the molecular density from 1.20 to 1.27 molecule.nm^{-2}.

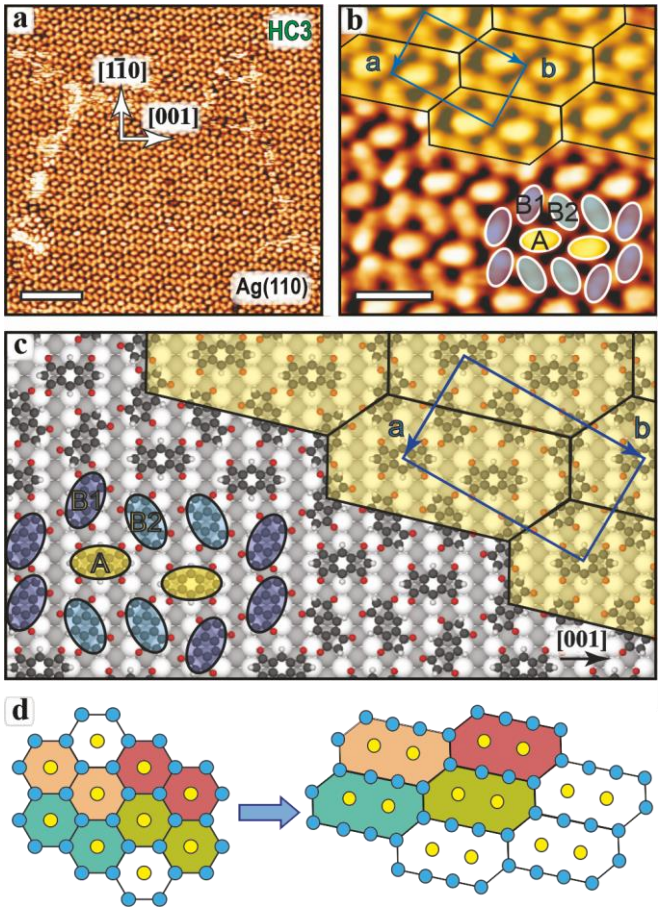

Figure 4: *(a,b) STM images of phase HC3 formed by $INDO_4$ on Ag(110). (c) Corresponding adsorption model. Ag atoms in the topmost close-packed rows are represented as light grey spheres and lower lying Ag atoms as dark grey. Scale bars: (a) 8 nm, (b) 2 nm. (d) Schematics illustrating the virtual transformation from a singly filled honeycomb pattern to a doubly filled.*

CONCLUSIONS

In summary, we have found three distinct phases of $INDO_4$ deposited at low coverage on the Ag(111), Ag(100) and Ag(110) surfaces. They exhibit complex unit cells and can be regarded as self-accommodating honeycomb framework. For all of them, the unit cell comprises six molecules exhibiting two distinct contrasts in STM. From a comparative study of the 3 different phases, we can postulate the following scenario. The supramolecular self-assembly represented by a self-accommodating honeycomb framework is stable and robust in terms of intermolecular interactions. Because it is also the result of a compromise with molecule-surface interactions, a change of the crystallographic phase of the surface induces a response in the molecular self-assembly. We showed that in this way we can induce a densification of the supramolecular phase, of up to 15%, with respect to the regular HC1 phase obtained on Ag(100). On Ag(110), a densification of 6% is produced by a lateral dimeric fusion of the honeycomb cavity. On Ag(111), a higher densification of 15% can be obtained thanks to an adequate registry with the substrate, however at the expense of a destabilization of 1/3 of the molecules and the appearance of a dynamic configuration at room temperature. The modifications of the molecule-substrate interactions are also reflected in the configuration of the edges of the different molecular islands. They are decorated by both type A and B for HC1 on Ag(100), suggesting a homogeneous relaxation inside the molecular layer. In contrary,

the domain edges are decorated by only type B for HC2 on Ag(111), or only type A for HC3 on Ag(110), thus reflecting the differentiation between these two adsorption configurations as a result of the molecular densification taking place in HC2 and HC3 phases. It should be mentioned that the presence of intrinsic Ag adatoms, that can be sometimes difficult to evidence,[29] could also eventually play a role in the different structures. Further work with theoretical modelling should help understanding the nature of the intermolecular interactions and the precise origin of the different behavior.

Experimental Section

The experiments were performed in ultra-high vacuum (UHV, base pressure in the low 10^{-10} mbar range). The single-crystal Ag(111), Ag(100) and Ag(110) surfaces were cleaned by several cycles of Ar^+ bombardment followed by annealing. INDO4 molecules were provided by Sigma-Aldrich as *rare and unique chemical*. The precursors were thoroughly degassed prior to deposition onto the atomically clean substrate held at room temperature (RT). The molecular powder was thermally sublimated from an evaporator heated to 150 °C for typical dosing time of 30 min. STM measurements were performed with a commercial Omicron VT-STM system operated at room temperature. The STM images were acquired in constant current mode with typical tunneling current $I_T \approx 0.3$ nA and sample bias $V_T \approx$ -(1–1.5) V. All images were subsequently calibrated using atomically resolved images of the pristine surfaces. Images were partly treated with the free software WSxM.[30]

SUPPORTING INFORMATION

Additional STM images.

ACKNOWLEDGEMENTS

F. Dumur and D. Gigmes are gratefully acknowledged for motivating this research field and anonymous reviewers for improving the quality of the manuscript. The project leading to this publication has received funding from Agence Nationale de la Recherche (ANR Grant N° ANR-17-CE08-0010 “DUALITY”).

References

(1) Barth, J. V. Molecular Architectonic on Metal Surfaces. *Annu. Rev. Phys. Chem.* **2007,** *58*, 375-407.

(2) Kudernac, T.; Lei, S. B.; Elemans, J.; De Feyter, S. Two-dimensional supramolecular self-assembly: nanoporous networks on surfaces. *Chem. Soc. Rev.* **2009,** *38*, 402-421.

(3) Dong, L.; Gao, Z. A.; Lin, N. Self-assembly of metal-organic coordination structures on surfaces. *Prog. Surf. Sci.* **2016,** *91*, 101-135.

(4) Brown, R. D.; Corcelli, S. A.; Kandel, S. A. Structural Polymorphism as the Result of Kinetically Controlled Self-Assembly. *Acc. Chem. Res.* **2018,** *51*, 465-474.

(5) Clair, S.; De Oteyza, D. G. Controlling a Chemical Coupling Reaction on a Surface: Tools and Strategies for On-Surface Synthesis. *Chem. Rev.* **2019,** *119*, 4717-4776.

(6) Jasper-Tonnies, T.; Gruber, M.; Ulrich, S.; Herges, R.; Berndt, R. Coverage-Controlled Superstructures of C-3-Symmetric Molecules: Honeycomb versus Hexagonal Tiling. *Angew. Chem. Int. Ed.* **2020,** *59*, 7008-7017.

(7) Zhang, L.; Zou, B.; Dong, D.; Huo, F. W.; Zhang, X.; Chi, L. F.; Jiang, L. Self-assembled monolayers of new dendron-thiols: manipulation of the patterned surface and wetting properties. *Chem. Commun.* **2001,** *19*, 1906-1907.

(8) Muller, K.; Enache, M.; Stöhr, M. Confinement properties of 2D porous molecular networks on metal surfaces. *J. Phys. Condens. Matter.* **2016,** *28*, 153003.

(9) Khan, S. B.; Lee, S. L. Supramolecular Chemistry: Host-Guest Molecular Complexes. *Molecules* **2021,** *26*, 3995.

(10) Cui, D.; MacLeod, J. M.; Ebrahimi, M.; Perepichka, D. F.; Rosei, F. Solution and Air Stable Host/Guest Architectures from a Single Layer Covalent Organic Framework. *Chem. Commun.* **2015,** *51*, 16510-16513.

(11) Stöhr, M.; Wahl, M.; Spillmann, H.; Gade, L. H.; Jung, T. A. Lateral manipulation for the positioning of molecular guests within the confinements of a highly stable self-assembled organic surface network. *Small* **2007,** *3*, 1336-1340.

(12) Zhang, H. M.; Xie, Z. X.; Long, L. S.; Zhong, H. P.; Zhao, W.; Mao, B. W.; Xu, X.; Zheng, L. S. One-step preparation of large-scale self-assembled monolayers of cyanuric acid and melamine supramolecular species on Au(111) surfaces. *J. Phys. Chem. C* **2008,** *112*, 4209-4218.

(13) Palma, C. A.; Bjork, J.; Rao, F.; Kuhne, D.; Klappenberger, F.; Barth, J. V. Topological Dynamics in Supramolecular Rotors. *Nano Lett.* **2014,** *14*, 4461-4468.

(14) Meier, D.; Adak, A. K.; Knecht, P.; Reichert, J.; Mondal, S.; Suryadevara, N.; Kumar, K. S.; Eguchi, K.; Muntwiler, M. K.; Allegretti, F.; et al. Rotation in an Enantiospecific Self-Assembled Array of Molecular Raffle Wheels. *Angew. Chem. Int. Ed.* **2021**, DOI:https://doi.org/10.1002/anie.202107708 https://doi.org/10.1002/anie.202107708, early access.

(15) Griessl, S.; Lackinger, M.; Edelwirth, M.; Hietschold, M.; Heckl, W. M. Self-assembled two-dimensional molecular host-guest architectures from trimesic acid. *Single Molecules* **2002,** *3*, 25-31.

(16) Ibenskas, A.; Simenas, M.; Kizlaitis, K. J.; Tornau, E. E. Trimesic Acid Molecule in a Hexagonal Pore: Central versus Noncentral Position. *J. Phys. Chem. C* **2019,** *123*, 3552-3559.

(17) Li, W.; Xu, S. L.; Chen, X. L.; Xu, C. Y. Structural transformations of carboxyl acids networks induced by concentration and oriented external electric field. *Chin. Chem. Lett.* **2021,** *32*, 480-484.

(18) Krief, P.; Becker, J. Y.; Ellern, A.; Khodorkovsky, V.; Neilands, O.; Shapiro, L. s-indacene-1,3,5,7(2H,6H)-tetraone ('Janus dione') and 1,3-dioxo-5,6-indane-dicarboxylic acid: Old and new 1,3-indandione derivatives. *Synthesis-Stuttgart* **2004,** *15*, 2509-2512.

(19) Sprick, R. S.; Thomas, A.; Scherf, U. Acid catalyzed synthesis of carbonyl-functionalized microporous ladder polymers with high surface area. *Polymer Chemistry* **2010,** *1*, 283-285.

(20) Sigalov, M.; Krief, P.; Shapiro, L.; Khodorkovsky, V. Inter- and intramolecular C-H...O bonding in the anions of 1,3-indandione derivatives. *Eur. J. Org. Chem.* **2008,** *4*, 673-683.

(21) Kalashnyk, N.; Salomon, E.; Mun, S. H.; Jung, J.; Giovanelli, L.; Angot, T.; Dumur, F.; Gigmes, D.; Clair, S. The Orientation of Silver Surfaces Drives the Reactivity and the Selectivity in Homo-Coupling Reactions. *ChemPhysChem* **2018,** *19*, 1802-1808.

(22) Kalashnyk, N.; Dumur, F.; Gigmes, D.; Clair, S. Molecular adaptation in supramolecular self-assembly: brickwall-type phases of indacene-tetrone on silver surfaces. *Chem. Commun.* **2018,** *54*, 8510-8513.

(23) Kalashnyk, N.; Mouhat, K.; Oh, J.; Jung, J.; Xie, Y.; Salomon, E.; Angot, T.; Dumur, F.; Gigmes, D.; Clair, S. On-Surface Synthesis of Aligned Functional Nanoribbons Monitored by Scanning Tunneling Microscopy and Vibrational Spectroscopy. *Nat. Commun.* **2017,** *8*, 14735.

(24) Bohringer, M.; Schneider, W. D.; Glockler, K.; Umbach, E.; Berndt, R. Adsorption site determination of PTCDA on Ag(110) by manipulation of adatoms. *Surf. Sci.* **1998,** *419*, L95-L99.

(25) Rochefort, A.; Vernisse, L.; Gomez-Herrero, A. C.; Sanchez-Sanchez, C.; Martin-Gago, J. A.; Cherioux, F.; Clair, S.; Coraux, J.; Martinez, J. I. Role of the Structure and Reactivity of Cu and Ag Surfaces in the Formation of a 2D Metal-Hexahydroxytriphenylene Network. *J. Phys. Chem. C* **2021,** *125*, 17333-17341.

(26) Palma, C. A.; Bjork, J.; Klappenberger, F.; Arras, E.; Kuhne, D.; Stafstrom, S.; Barth, J. V. Visualization and thermodynamic encoding of single-molecule partition function projections. *Nat. Commun.* **2015,** *6*, 6210.

(27) Karamzadeh, B.; Eaton, T.; Torres, D. M.; Cebula, I.; Mayor, M.; Buck, M. Sequential nested assembly at the liquid/solid interface. *Faraday Discuss.* **2017,** *204*, 173-190.

(28) Griessl, S. J. H.; Lackinger, M.; Jamitzky, F.; Markert, T.; Hietschold, M.; Heckl, W. M. Room-temperature scanning tunneling microscopy manipulation of single C-60 molecules at the liquid-solid interface: Playing nanosoccer. *J. Phys. Chem. B* **2004,** *108*, 11556-11560.

(29) Blowey, P. J.; Velari, S.; Rochford, L. A.; Duncan, D. A.; Warr, D. A.; Lee, T. L.; De Vita, A.; Costantini, G.; Woodruff, D. P. Re-evaluating how charge transfer modifies the conformation of adsorbed molecules. *Nanoscale* **2018,** *10*, 14984-14992.

(30) Horcas, I.; Fernández, R.; Gómez-Rodríguez, J. M.; Colchero, J.; Gómez-Herrero, J.; Baro, A. M. WSXM: A software for scanning probe microscopy and a tool for nanotechnology. *Rev. Sci. Inst.* **2007,** *78*, 013705.

TOC GRAPHICS